Journal of Fluorine Chemistry 222–223 (2019) 75–80

Contents lists available at ScienceDirect

Journal of Fluorine Chemistry

journal homepage: www.elsevier.com/locate/fluor

Optical and calorimetric studies of K_2TaF_7

Svetlana V. Mel'nikova[a], Evgeniy V. Bogdanov[a,b,*], Maxim S. Molokeev[a,c,d], Natalia M. Laptash[e], Igor N. Flerov[a,c]

[a] Kirensky Institute of Physics, Federal Research Center KSC SB RAS, 660036 Krasnoyarsk, Russia
[b] Institute of Engineering Systems and Energy, Krasnoyarsk State Agrarian University, 660049 Krasnoyarsk, Russia
[c] Institute of Engineering Physics and Radioelectronics, Siberian Federal University, 660074 Krasnoyarsk, Russia
[d] Department of Physics, Far Eastern State Transport University, Khabarovsk, 680021, Russia
[e] Institute of Chemistry, Far Eastern Department of RAS, 690022 Vladivostok, Russia

ARTICLE INFO

Keywords:
Phase transition
Ferroelasticity
Optical properties
Photoelasticity
Heat capacity
Entropy

ABSTRACT

Optical and calorimetric experiments on K_2TaF_7 are performed in a wide temperature range. No features were found in the behavior of the birefringence $\Delta n_b(T)$, the angle of rotation of the indicatrix $\phi(T)$ and the heat capacity $\Delta C_p(T)$ except for those associated with the $Pnma \leftrightarrow P2_1/c$ phase transition. Structural transformation was characterized as strong first order "proper" ferroelastic accompanied by a huge angle $\phi \approx 40^\circ$ and strong pretransition phenomena in $\Delta n_b(T)$. Two contributions to the anomalies of the optical properties were found associated with the photoelastic effect and the transition parameter related linearly to the spontaneous deformation. Thermal treatments cause correlated changes in temperature and enthalpy of the phase transition, which leads to the invariance of the large magnitude of the corresponding entropy $\Delta S = 22$ J/mol·K which does not match the model with the absence of structural disorder in the *Pnma* phase.

1. Introduction

Potassium heptafluorotantalate, K_2TaF_7, is an important intermediate material in the commercial production of high-purity tantalum metal [1,2]. It belongs to the series of complex fluorides with the general chemical formula A_2MF_7 which can crystallize in different crystallographic modifications depending on the size of monovalent cation A and central atom M [3]. It is believed that in most of these compounds the seven-coordinated $[MF_7]^{2-}$ anionic complex exists in the form of mono-capped trigonal prism with C_{2v} symmetry. At the same time, the shape of anionic complex in the form of pentagonal bipyramid with D_{5h} symmetry was revealed in A_2BiF_7 and A_2SbF_7 compounds through vibration spectroscopy experiments and "ab initio" calculations of the electronic structure [4].

At room temperature, the symmetry of the crystal lattice of heptafluorides A_2TaF_7 is tetragonal ($P4/nmm$, $Z = 2$) [5] or monoclinic ($P2_1/c$, $Z = 4$) [2,3] when $A =$ Rb, $NH_4$and K, respectively. All of them are known to undergo successive or unique phase transitions: $(NH_4)_2TaF_7$ – $P4/nmm(T_1 = 174\ K) \leftrightarrow Pmmn(T_2 = 156\ K) \leftrightarrow$ tetragonal [6], Rb_2TaF_7 – $P4/nmm$ ($T_0 = 145\ K$) $\leftrightarrow Cmma$ [7], K_2TaF_7 – $P2_1/c$ ($T_0 = 475\ K$) $\leftrightarrow Pnma(Z = 4)$ [2,3].

Rather different entropy parameters, ΔS, of ferroelastic structural transformation $P4/nmm \leftrightarrow Pmmn$ were found in two former substances: $0.3R$ and $0.5R$, respectively. It was assumed that this point can be associated with more pronounced anharmonicity of critical vibrations of the tetrahedral cation NH_4^+ compared with the spherical Rb^+ cation. In accordance with the small entropy change $\Delta S_2 = 0.2R$, the low temperature transformation in rubidium compound was characterized as transition of the displacive type associated with the small shifts of atoms from the equilibrium positions in the initial $P4/nmm$ phase [7]. Contrary to these results, phase transition in K_2TaF_7 was accompanied by rather large entropy change $\Delta S = 15.4$ J/mol·K $\approx R$·ln6 which is characteristic for order-disorder transformations [8,9]. However, analysis of structural data showed that in the high-temperature phase there is no disordering of any structural units. Thus, mechanism of structural distortions in potassium heptafluorotantalate is rather intriguing. The nature of the phase transition in K_2TaF_7 was not studied in details. At high temperatures, this heptafluoride shows three additional thermal effects at the temperatures 998 K, 1022 K and 1048 K which were supposed to be related to a solid-solid transition to hypothetical γ-form, incongruent melting, and mixing of two liquids, respectively [8]. Very high and close values of these specific temperatures prevent to detail study of nature of the phenomenon observed.

Despite the large number of investigations devoted to K_2TaF_7, the

* Corresponding author at: Kirensky Institute of Physics, Federal Research Center KSC SB RAS, 660036 Krasnoyarsk, Russia.
E-mail address: evbogdanov@iph.krasn.ru (E.V. Bogdanov).

https://doi.org/10.1016/j.jfluchem.2019.04.016
Received 18 January 2019; Received in revised form 24 April 2019; Accepted 24 April 2019
Available online 25 April 2019
0022-1139/

results obtained are limited in the most cases to X-ray, Raman and NMR studies [2,8–15]. The temperature behavior of various physical properties has not been sufficiently studied. However, investigations of this kind in a wide temperature range and in the vicinity of the phase transition *Pnma* ↔ $P2_1/c$ undergoing by heptafluorotantalate are very useful because they will shed light on the nature and mechanism of the distortions of the structure. For this purpose, in the present paper, we performed polarization-optical studies, measurements of heat capacity, angle of rotation of the optical indicatrix, and birefringence in a wide temperature range. We limited our research to only α ↔ β transformation due to very high temperature of β ↔ γ transition (T = 998 K) and limited temperature capabilities of the measuring equipment (T ≈ 850 K).

2. Experimental

2.1. Synthesis, growth and X-ray inspection of samples

The preparation method of potassium heptafluorotantalate K_2TaF_7 is based on its precipitation from hydrofluoric acid solutions. This compound is poorly soluble and crystallizes in the form of transparent birefringent needles [2]. Tantalum oxide Ta_2O_5 of a reagent grade was used as a starting material. It was dissolved in concentrated HF (˜ 40% wt) at heating followed by addition of any potassium salt (KF, KHF_2or KCl). For example, m ≈ 10 g Ta_2O_5 were dissolved in V ≈ 30–40 ml of concentrated HF at heating in a platinum or glass-carbon plate. The obtained solution was diluted by water and a stoichiometric quantity of potassium salt was added in accordance with the reaction: H_2TaF_7 + 2·KCl = K_2TaF_7 + 2·HCl. It should be noted that a plentiful precipitate of small transparent needles is formed under virtually any ratio of the initial reagents. The crystalline precipitate was filtered off and washed under vacuum with alcohol. Slow evaporation of the mother liquor in the air or recrystallization from HF solutions resulted in larger single crystals of K_2TaF_7. The composition of the crystals was checked using EDX and XPS methods. Both indicated the oxygen presence, so the fluorine amount was determined by a fluoride ion-selective electrode calibrated with different diluted solutions of standard NaF. The powder was decomposed with $NaKCO_3$ at temperature T = 900 °C during at t = 30 min, and the cake was leached with hot water and filtered. The solution pH was then adjusted to 5 – 6. The fluorine amount was deduced from six measurements with standard solutions containing different fluorine concentrations. The fluorine content was 31.5 ± 0.4% (compared to the calculated 33.92% for K_2TaF_7), which means the composition of $K_2TaO_{0.3}F_{6.4}$. To make sure that such an amount of oxygen impurity does not affect the type of structure, X-ray studies were performed.

The powder diffraction data of $K_2TaO_{0.3}F_{6.4}$ for Rietveld analysis was collected at room temperature with a Bruker D8 ADVANCE powder diffractometer (Cu-Kα radiation) and linear VANTEC detector. The step size of 2θ was 0.016°, and the counting time was 0.3 s per step. Rietveld refinement was performed by using TOPAS 4.2 [16]. All peaks were indexed by monoclinic cell $P2_1/c$ with parameters close to previously found for K_2TaF_7 [10,11]. This crystal structure (Fig. 1) was taken as starting model for Rietveld refinement which was found to be stable revealing low R-factors (Table 1, Fig. 1 *a*). These results allow us to use the stoichiometric formula K_2TaF_7.

2.2. Optical observations

Optical studies were performed using a polarizing microscope Axioskop-40 and two Linkam temperature chambers: LTS 350 and TS 1500. The temperature investigations were carried out in a quasi-static mode with an accuracy of ± 0.1 K in the range of 100–850 K. The extinction position and the angle of rotation of the indicatrix were determined with an accuracy of 0.5°. The birefringence was measured using a Berek compensator Leica with an accuracy of ≈ 0.00001.

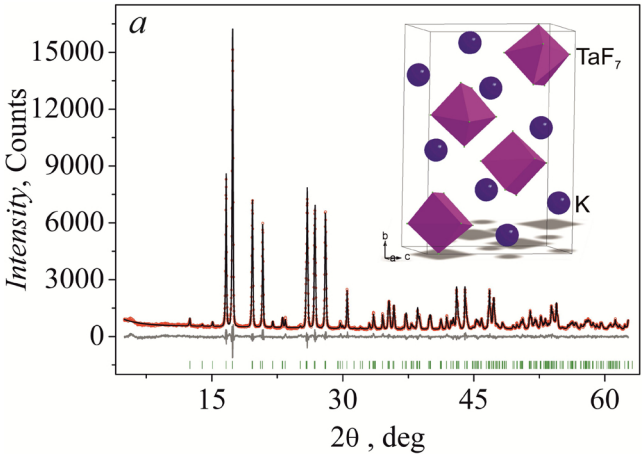

Fig. 1. (*a*) Difference Rietveld plot and crystal structure of K_2TaF_7.

Table 1
Main parameters of processing and refinement of the K_2TaF_7 sample.

Compound	K_2TaF_7
Sp.Gr.	$P2_1/c$
a, Å	5.8613 (1)
b, Å	12.7190 (2)
c, Å	8.5231 (2)
β, °	90.178 (2)
V, Å^3	635.39 (2)
Z	4
2θ-interval, °	5-62
R_{wp}, %	5.81
R_p, %	4.64
R_{exp}, %	3.56
χ^2	1.63
R_B, %	1.81

Grown samples of K_2TaF_7 are very small needle crystals with a thickness of 50–100 μm and a length of up to 1000 μm similar to those obtained in [2]. In the cross-section, these crystalline formations have the shape of a hexahedron (pencil) and consist of six blocks-twins with an exit of the [010] axis on the faces. The direction [100] is located along the length of the sample. During microscopic studies, the crystals were installed on one of the six faces (010), so the light propagated along [010] and therefore oblique extinction in polarized light was always observed.

The samples with the most developed pair of opposite faces and a good extinction were selected for experiments. Measurements of the angle of rotation of the optical indicatrix $\phi(T)$, and birefringence $\Delta n_b(T)$ were carried out simultaneously on very thin samples d≈ 40 μm in the temperature range 100–850 K.

At room temperature, an "oblique" extinction of the samples with a giant ϕ ≈ 30° angle of rotation of the indicatrix around [010] was observed. During heating, this angle gradually decreases. However, at $T_{0\uparrow}$ ≈ 500 K (498 — 508 K for different samples), the crystal undergoes a phase transition accompanied by a strong explosive-like cracking of the sample. Only in rare cases, the samples may partially retain their shape, and then measurements in the high-temperature phase are possible. Just above the transition region (T – T_0 = 0–7 K), the crystal becomes strongly compressed and does not show extinctions and anisotropy. With further heating, a "direct" extinction ϕ ≈ 0° of the orthorhombic phase is formed. Upon cooling, this extinction exists until the transition temperature $T_{0\downarrow}$ = (463 – 453) K to the low-temperature phase, revealing giant temperature hysteresis δT_0≈ 45 K. At $T_{0\downarrow}$, the sample finally decays into very small parts. A similar situation with a destruction of the K_2TaF_7 sample at heating above T_0 was observed in

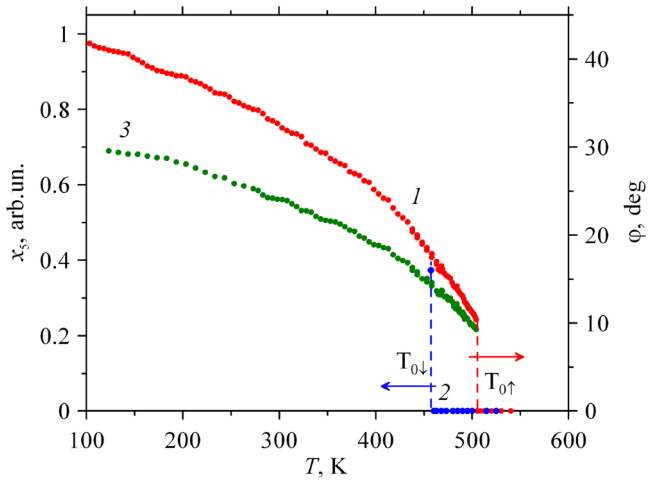

Fig. 2. Temperature dependences of the angle ϕ(*T*) of optical indicatrix rotation around [010] in the heating (*1*) and cooling (*2*) modes and of the quantity of $\Delta n_b \cdot \sin 2\varphi \sim x_5$ (*3*) for the K_2TaF_7 crystal.

the single-crystal X-ray experiments at $T \approx 509$ K [15]. In addition, monolithic single crystal K_2TaF_7 grown from the melt will necessarily be destroyed when cooled through a phase transition due strong volume change [2].

The temperature dependence of the angle of rotation of the optical indicatrix ϕ(*T*) is shown in Fig. 2 (curve 1). Upon cooling down to 100 K, no anomalous behaviour of ϕ(*T*) was observed. At $T = 100$ K, the angle of rotation reaches $\phi \approx 42^\circ$ and does not show a saturation. Upon heating, ϕ gradually decreases and then abruptly go down to $\phi = 0$ at $T = T_{0\uparrow}$.

The birefringence measurements with the Berek compensator were always performed in the direction of the principal axes of the optical indicatrix. Therefore, at each temperature point, the sample was oriented in accordance with the angle of rotation φ (Fig. 2). This fact, combined with a slight anisotropy of fluoride crystal, a small sample thickness and blockness of the sample, creates a rather large error in the determination of the absolute value of birefringence. The temperature behavior of the birefringence $\Delta n_b(T)$ is shown in Fig.3*a*. The crystal is characterized by a weak optical anisotropy and an unusual temperature dependence of birefringence. When heated, the birefringence gradually decreases from the value $\Delta n_b = (n_c - n_a) \approx 0.007$ at $T = 100$ K to $\Delta n_b \approx 0.006$ at $T = 400$ K. In the temperature range of $T = 400$–500 K, as T_0 was approached, an increase in the value of Δn_b was observed followed by a sharp decrease and destruction of the samples at T_0. The $P2_1/c \leftrightarrow Pnma$ phase transition occurs in different samples in different ways. Most often, the crystals explode and leave the field of view of the microscope. The thin and uniformly extinguish plates most successfully pass through the phase transition. In a narrow temperature range above the transition temperature $T - T_0 = (0–7)$ K for different samples there is no extinction of the sample due to strong and inhomogeneous deformations, consequently, the plate looks isotropic $\Delta n \approx 0$. Over time or when heated, optical anisotropy appears again, reaching value of $\Delta n \approx 0.003$. In the temperature range $T = 650$–850 K, a linear dependence of $\Delta n(T)$ is observed.

2.3. Calorimetric study

The measurements of the heat capacity, $C_p(T)$, of the K_2TaF_7 crystal were carried out over a wide temperature range from $T = 100$–620 K in heating and cooling modes using differential scanning microcalorimeter DSM-10 M. Powdered sample with a mass about 0.2 g was put into an aluminum sample holder. The heat flow through the sample and reference compound Al_2O_3 was recorded versus temperature.

Upon cooling up to $T \approx 100$ K, the anomalous behavior of the heat capacity was not observed. Above room temperature, calorimetric studies were performed in two stages. At the first stage – *A*, measurements were carried out up to $T \approx 530$ K, and at the second – *B* up to $T \approx 620$ K. In both cases, reproducible anomaly of heat capacity was observed during thermal cycling. After elimination of the lattice contribution, C_{lat}, from the experimental data $C_p(T)$, the information on excess heat capacity, $\Delta C_p = C_p - C_{lat}$, associated with the phase transition $Pnma \leftrightarrow P2_1/c$ was obtained. Fig. 4*a* shows the temperature dependence of ΔC_p measured in heating (*1*) and cooling (*2*) modes for option *A*. At thermal cycling rate equal to $dT/dt = 16$ K/min, the peaks of ΔC_p corresponded to phase transition temperature were found at $T_{0\uparrow} = 485 \pm 1$ K and $T_{0\downarrow} = 426 \pm 1$ K upon heating and cooling, respectively. Thus, transformation $Pnma \leftrightarrow P2_1/c$ is of the strong first order with a gigantic temperature hysteresis $\delta T_0 \approx 46$ K which coincides with the value observed in optical measurements above.

In order to determine the hysteresis corresponding to the equilibrium conditions, dependence of temperature T_0 on the heating/cooling rate was studied in a wide range of the value $dT/dt = \pm$ (2–16) K/min (Fig. 4*b*). The dependences $T_{0\uparrow}((dT/dt)^{1/2})$ and $T_{0\downarrow}((dT/dt)^{1/2})$ were found linear. Extrapolation of these lines to $dT/dt = 0$ allows one to obtain the real values of temperature of the phase transition $T_{0\uparrow} = 458$ K, $T_{0\downarrow} = 445$ K and as result a strong decrease in the thermal hysteresis $\delta T_0 \approx 13$ K.

The enthalpy change associated with the phase transition, $H = \int \Delta C_p(T) \cdot dT = 10{,}000 \pm 700$ J/mol, was evaluated by integration of temperature dependence of excess heat capacity determined by measurements in heating mode.

The results obtained at the stage *B* of measurements in several thermal cycles, for example $N = 1$–7, are shown in Fig. 5. One can see, that during cyclic heating and cooling in the range of $T = 330$–620 K at

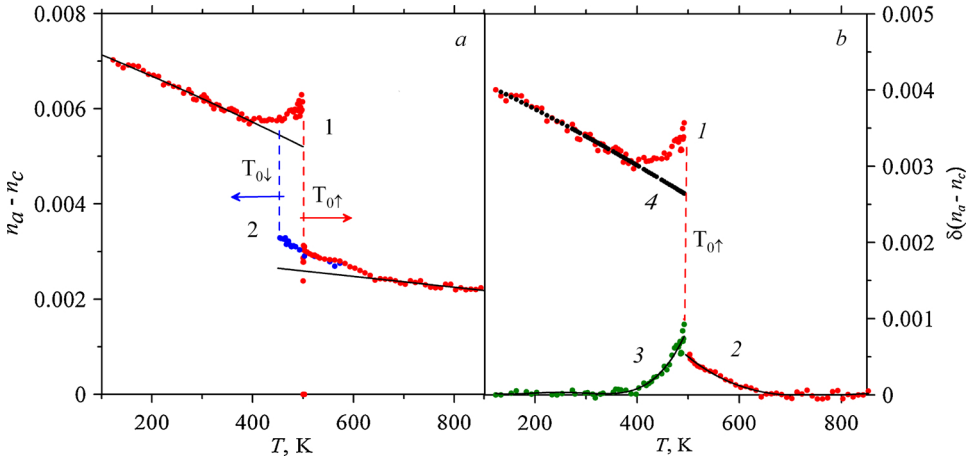

Fig. 3. (*a*) Temperature behavior of the birefringence $\Delta n_b(T) = (n_a - n_c)(T)$ in K_2TaF_7 in the heating (*1*) and cooling (*2*) processes. (*b*) Temperature dependence of the anomalous component of the birefringence $\delta(n_a - n_c)$ (*1*, *2*) and the fluctuation contribution to $\delta(n_a - n_c)$ above (*1*), and below (*3*) temperature of the phase transition T_0. The component of the birefringence associated with the transition parameter (*4*.

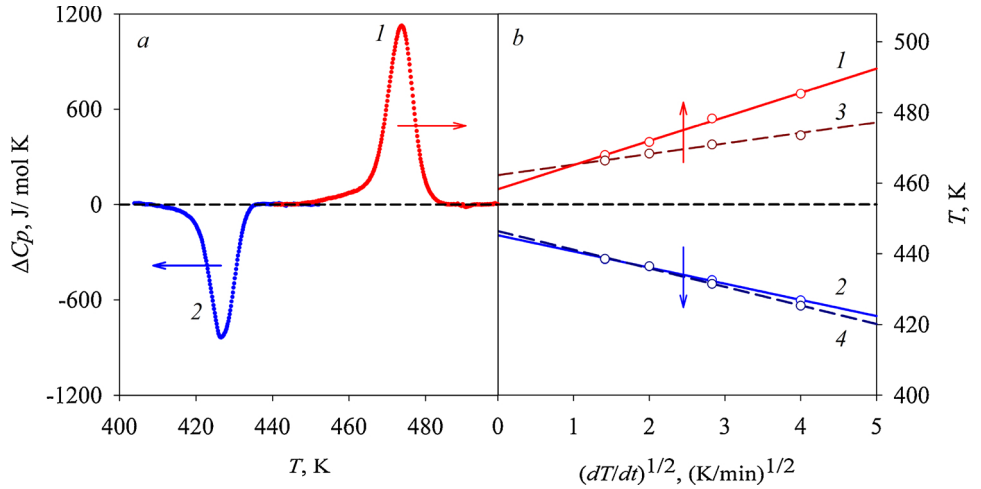

Fig. 4. (*a*) Anomalous heat capacity measured at the stage *A* in the heating (*1*) and cooling (*2*) modes at constant rate of the temperature change $dT/dt = \pm 16$ K/min. (*b*) Dependence of the phase transition temperature on the rate of heating and cooling at the stages *A* (solid lines *1*, *2*) and *B* (dashed lines *3*, *4*).

the constant rate $dT/dt = 16$ K/min, K_2TaF_7 demonstrates rather significant hysteretic phenomena in the vicinity of the phase transition. The peaks of the anomalous heat capacity are shifted and changed in the area which is associated with the enthalpy of the phase transition, ΔH (Fig. 5*a–c*).

The phase transition temperature in a heating mode was also found strongly dependent on *N* decreasing rather strong during the first three cycles and increasing then step by step to stable value (Fig. 5*c*). However, upon cooling, T_0 impacts unusual behaviour remaining almost constant in all series of measurements. On the one hand, one can assume that such a peculiarity is most likely related to the temperature limit of the *Pnma* phase existence on cooling. On the other hand, it means that the value of the thermal hysteresis δT_0 depends only on $T_0\uparrow$.

After all thermal cycles of the heat treatment at the stage *B* at the rate $dT/dt = 16$ K/min and stabilization of temperature of the phase transition T_0, the thermal hysteresis δT_0 depending on the heating/cooling rate was also studied. The results of these experiments are shown in Fig. 4*b* by dashed lines (*3*) and (*4*). It is seen that both dependences, $T_0\uparrow((dT/dt)^{1/2})$ and $T_0\downarrow((dT/dt)^{1/2})$, are also linear. Moreover, the behaviour of $T_0\downarrow$ similar to observed at the stage *A*. However, in the heating mode, a slope of the $T_0\uparrow(dT/dt)$ line is less in comparison to data of the stage *A*. As a result of extrapolation of the experimental dependence $T_0((dT/dt)^{1/2})$ to quasi-equilibrium conditions $dT/dt = 0$ leads to the different thermal parameters: $T_0\uparrow = 462$ K, $T_0\downarrow = 445$ K and $\delta T_0 \approx 17$ K.

3. Discussion

First of all, it is necessary to pay attention on rather large difference in temperature of the phase transition observed in calorimetric and optical measurements. We can assume at least three reasons for the phenomenon observed. First is associated with the different experimental conditions: measurements of heat capacity were performed in dynamical mode with a high rate of the temperature change while optical observations were carried out in a quasi-static mode. The second reason is that powder and single crystal samples have a rather different volume for the in calorimetric ($V \approx 70\,mm^3$) and optical ($V \approx 10^{-2}\,mm^3$) experiments, respectively. Finally, the most important circumstance is the difference in the state of the samples in the measurement processes. The powder samples were stressed due to pressing in the container and single crystals were stress-free.

In addition to the transition at $T_0 \approx 500$ K, some features were found below $T \approx 150$ K in the NMR and Raman spectra of the K_2TaF_7 crystal associated with a change in the symmetry of the anionic $[TaF_7]^{2-}$ polyhedron from C_1 to C_{2v} [11–13]. Optical and calorimetric studies performed in the present work in a wide temperature range did not reveal any anomalies in the behavior of $\Delta n(T)$ and $\varphi(T)$, and $\Delta C_p(T)$ below T_0. Both experiments confirmed the strong first order of the $P2_1/c \leftrightarrow$ *Pnma* transformation accompanied by giant thermal hysteresis $\delta T_0 \approx 45$ K.

Due to the lowering of symmetry below the transition temperature, a component of the shear spontaneous deformation x_5 appears in the monoclinic phase causing the optical indicatrix turn by angle $\phi \approx 40^\circ$ around [010]. Such a huge angle of rotation of the indicatrix is typical of the "proper" ferroelastic transitions observed, for example, earlier in $CsLiSO_4$ and $CsLiCrO_4$ [17–19], where the transition parameter η is linearly related to x_5. In the case of small angles of rotation of the indicatrix and weak temperature-induced birefringence variations, one may expect the proportionality $x_s(T) \sim \Pi(T)$, as it was found for $RbMnCl_3$ [20]. However, due very large value of φ in K_2TaF_7, the dependence $\Pi(T)$ does not reflect the behavior of $x_5(T)$.

By transforming the tensor of polarization constants a_{ij} to the

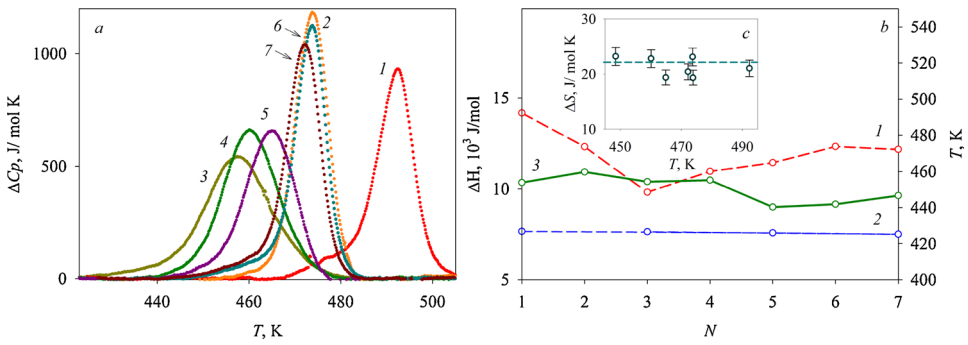

Fig. 5. (*a*) Results of measurements at the stage *B* over seven thermal cycles *N* = (1–7), at a rate $dT/dt = \pm 16$ K/min. Temperature behaviour of anomalous heat capacity in the heating modes. (*b*) Dependence of the phase transition temperature on *N* in heating (*1*) and cooling (*2*) modes and excess enthalpy measured in the heating mode (*3*). (*c*) Temperature dependence of the excess entropy during all thermal cycling.

reference frame that changes its orientation with temperature, we obtain $\sin(2\phi) = n_{av}^3 \cdot p_{55} \cdot x_5 / \Delta n_b$, where n_{av} is the averaged refractive index and p_{55} is the coefficient of the photoelastic effect. This suggests that the deformation should be related to the angle of rotation of the optical indicatrix by a complex relationship $x_5 \sim \Delta n_b \cdot \sin(2\phi)$, the temperature behavior of which is plotted in Fig. 2 curve (*3*).

Using the results of the present work and previous studies [2,10,11], one can estimate the value of p_{55} at room temperature. The calculation, performed using the relationship $x_5 = \Delta n_b \cdot \sin(2\phi)/n^3 \cdot p_{55}$ and values $n_{av} = 1.41$ [2], $x_5 = \mathrm{tg}(\beta - 90) = 0.004$ [11], $\phi = 30^\circ$, $\Delta n_b = 0.006$ shows a very high value $p_{55} \approx 0.46$. For comparison, in $CsLiSO_4$, the coefficient of the photoelastic effect is almost ten times less ($p_{66} = 0.05$) [19].

The behavior of the anomalous component of the birefringence $\delta n_b = \delta(n_c - n_a)$ of the K_2TaF_7 crystal is presented in Fig. 3*b* (*1*, *2*). The dependence $\delta n_b(T)$ was obtained by subtracting the linear temperature dependence of the birefringence (extrapolated from the orthorhombic phase) out of the dependence $\Delta n(T)$ depicted in Fig. 3. As can be seen, the pre-transition effects are observed over a wide temperature range ($T - T_0 \approx 100$ K) above the phase transition temperature. At temperatures close to T_0, the anomalous component of the birefringence governed by the pre-transition phenomena reaches ~ 20% of the total anomaly (Fig. 3*b*).

The fluctuation contribution of the transition parameter to the birefringence (Fig. 3*b*) can be extracted under the assumption that the temperature dependences of the fluctuation components of the birefringence anomaly in *Pnma* (*2*), and $P2_1/c$ phases (*3*) are symmetric with respect to the phase transition temperature T_0 by analogy with the effects observed for some other crystals [21,22]. The decomposition of the birefringence anomaly near T_0 into the fluctuation component and the component associated with the transition parameter for the K_2TaF_7 crystal is shown in Fig. 3b (*4*). Similar large pre-transition effects were also revealed in the "proper" ferroelastics, $CsLiSO_4$ and $CsLiCrO_4$, with the transformations of the order-disorder type [18].

Hysteretic phenomena observed in calorimetric experiments at stages *A* and *B* can be considered as associated with the effect of annealing the sample when heated well above the transition temperature. A strong change in the δT_0 value during the thermal cycling at the stage *B* at constant dT/dt means that the closeness of the transformation *Pnma*↔ $P2_1/c$ to the tricritical point ($\delta T_0 = 0$) is also changed. However, the decrease/increase of the temperature T_0 in a heating mode correlates with decrease/increase in the enthalpy of the phase transition, ΔH (Fig. 5*c*). As a result the entropy change, associated with both parameters, $\Delta S \approx \Delta H/T_0$, and determined by integration of the $(\Delta C_p/T)(T)$ function, remains almost unchanged during all thermal cycles, $\Delta S = 22 \pm 2$ J/mol·K $\approx R \cdot \ln 14$ (Fig. 5*d*).

On the one hand, the constancy of entropy observed during thermal cycling means that thermal treatment does not effect on a character of structural distortions, i.e. on the mechanism of the phase transition. On the other hand, rather large value of the excess entropy clearly indicates that the corresponding distortions of the structure are associated with either order-disorder or reconstructive processes as it was found for example in double fluoride salts $(NH_4)_2MF_6 \cdot NH_4F$ (*M*: Ge, Ti, Sn) [23–25]. However, firstly, the disorder of any structural elements were not observed in the initial high temperature phase of K_2TaF_7 [15] and, secondly, the symmetries *Pnma* and $P2_1/c$ are related by the group-subgroup relation, which is not typical for reconstructive phase transitions. Nevertheless, X-ray studies revealed abnormally large displacements of fluorine atoms in phase $P2_1/c$, resulting in a ~ 1.2 times change in the $[TaF_7]^{2-}$ polyhedron volume and a change in the coordination number of potassium atoms from 9 to 10 [15]. It can be assumed that such strong changes in the structure can be a cause of a large change in the entropy. However, at this stage it is impossible to propose a model that allows one to estimate the corresponding value of ΔS.

As it was shown above, K_2TaF_7 undergoes "proper" ferroelastic phase transition. In such a case the function $(\Delta n_b \cdot \sin(2\varphi))(T)$ is proportional to the shear component of the spontaneous deformation x_5 (Fig. 2) associated with the order parameter η. On the other hand, the entropy of the phase transition is related to the order parameter as follows: $\Delta S \sim \eta^2$ [26]. Fig. 2 shows a strong change in $x_5 \sim \eta$ in a wide temperature range. Thus, the excess heat capacity as well as entropy should also exist far below T_0. The entropy of the phase transition measured in the present paper exceeds the value of previously reported $\Delta S = 15.4$ J/mol·K $\approx R \cdot \ln 6$ [8,9]. However, in both cases, the integration of the function $(\Delta C_p/T)(T)$ was performed in a rather narrow temperature range, $T \approx T_0 \pm 25$ K, where excess heat capacity was detected (Fig. 4*a*). It is necessary to point out that DSM method provides reliable information on the values of the excess heat capacity as well as entropy only near the phase transition point. Thus, one can assume that the real value of ΔS can be even higher. To test the validity of this assumption, calorimetric measurements using of high sensitive calorimeters are needed.

4. Conclusions

Studies of optical properties and heat capacity of K_2TaF_7 performed in a wide temperature range allowed us to establish the following important points.

In phase $P2_1/c$, below T_0, no anomalies were detected in the dependences $\varphi(T)$, $\Delta n_b(T)$ and $\Delta C_p(T)$. Thus, features observed in the NMR and Raman spectra are not related to phase transitions.

It is found that the phase transition *Pnma*↔$P2_1/c$ is a pronounced first-order transformation, accompanied by a giant thermal hysteresis and explosion-like destruction of single crystals.

A huge angle of rotation of the indicatrix $\phi \approx 40^\circ$ and strong pre-transition phenomena in the birefringence above and below T_0 show that K_2TaF_7 undergoes a "proper" ferroelastic phase transition. The anomalies in the optical properties associated with the phase transition cannot be described by the photoelastic effect only through shear deformation. There is an additional contribution from the transition parameter which is related linearly to the spontaneous deformation.

The strong effect of heat treatments on the correlated changes in temperature and enthalpy of the phase transition was found, which, however, does not affect the magnitude of the change in entropy. The very large entropy of the phase transition, $\Delta S \approx R \cdot \ln 14$, does not match the model with the absence of structural disorder in phase *Pnma* [15] and can only be assumed to be associated with a giant change in the volume of the anionic polyhedron and change in coordination number the K^+ cations.

Acknowledgements

The reported study was funded by RFBR according to the research project № 18-02-00269.

References

[1] A. Agulyansky, The Chemistry of Tantalum and Niobium Fluoride Compounds, Elsevier, 2004, p. 407.
[2] A. Agulyansky, Potassium fluorotantalate in solid, dissolved and molten conditions, J. Fluorine Chem. 123 (2003) 155–161.
[3] Z. Mazej, R. Hagiwara, Hexafluoro-, heptafluoro-, and octafluoro-salts, and [MnF5n +1] (n = 2, 3, 4) polyfluorometallates of singly charged metal cations, Li+ –Cs+, Cu+, Ag+, In+ and Tl+, J. Fluorine Chem. 128 (2007) 423–437.
[4] G.W. Drake, D.A. Dixon, J.A. Sheehy, J.A. Boatz, K.O. Christe, Seven-coordinated pnicogens. Synthesis and characterization of the SbF_7^{2-} and BiF_7^{2-} dianions and a theoretical study of the AsF_7^{2-} dianion, J. Am. Chem. Soc. 120 (1998) 8392–8400.
[5] N.M. Laptash, A.A. Udovenko, T.B. Emelina, Dynamic orientation disorder in rubidium fluorotantalate. Synchronous Ta-O and Ta-F vibrations, J. Fluorine Chem. 132 (2011) 1152–1158.
[6] E. Pogoreltsev, S.V. Mel'nikova, A.V. Kartashev, M.S. Molokeev, M.V. Gorev, I.N. Flerov, N.M. Laptash, Ferroelastic phase transitions in $(NH_4)_2TaF_7$, Phys. Solid State 55 (2013) 611–618.
[7] E.I. Pogorel'tsev, S.V. Mel'nikova, A.V. Kartashev, M.V. Gorev, I.N. Flerov, N.M. Laptash, Thermal, optical, and dielectric properties of fluoride Rb_2TaF_7, Phys.

Solid State 59 (2017) 986–991.
[8] L. Kosa, I. Macková, I. Proks, O. Pritula, L. Smrčok, M. Boča, H. Rundlőf, Phase transitions of K_2TaF_7 within 680–800°C, Cent. Eur. J. Chem. 6 (2008) 27–32.
[9] M. Boča, A. Rakhmatullin, J. Mlynáriková, E. Hadzimová, Z. Vaskováa, M. Miušíkc, Differences in XPS and solid state NMR spectral data and thermo-chemical properties of iso-structural compounds in the series $KTaF_6$, K_2TaF_7 and K_3TaF_8 and $KNbF_6$, K_2NbF_7 and K_3NbF_8, Dalton Trans. 44 (2015) 17106–17117.
[10] J.L. Hoard, Structures of complex f1uorides. Potassium heptafluocolumbate and potassium heptafluotantalate. The configuration of the heptafluocolumbate and heptafluotantalate ions, J. Am. Chem. Soc. 61 (1939) 1252–1259.
[11] C.C. Torardi, L.H. Brixner, G. Blasse, Structure and luminescence of K_2TaF_7 and K_2NbF_7, J. Solid State Chem. 67 (1987) 21–25.
[12] E.C. Reynhardt, J.C. Pratt, A. Watton, H.E. Petch, NMR study of molecular motion and disorder in K_3ZrF_7 and K_2TaF_7, J. Phys. C: Solid State Phys. 14 (1981) 4701–4715.
[13] R.B. English, A.M. Heyns, E.C. Reynhardt, An x-ray, NMR, infrared and Raman study of K_2TaF_7, J. Phys. C: Solid State Phys. 16 (1983) 829–840.
[14] A. Agulyansky, V. Bessonova, V. Kuznetsov, N. Sklokina, Subsolidus polymorphism of potassium heptafluorotantalate, Zh. Neorg. Khim. 27 (1982) 679–682.
[15] V. Langer, L. Smrcok, M. Boca, Dipotassium heptafluorotantalate (V), β-K_2TaF_7, at 509 K, Acta Cryst E62 (2006) i91–i93.
[16] Bruker AXS, TOPAS V4: General Profile and Structure Analysis Software for Powder Diffraction Data. – User's Manual, Bruker AXS, Karlsruhe, Germany, 2008.
[17] K.S. Aleksandrov, S.V. Mel'nikova, A.I. Kruglik, S.M. Tret'yak, V.V. Mitkevich, X-ray diffraction and optical studies of the phase transition in the $CsLiCrO_4$ crystal, Kristallografiya 34 (1989) 147–153 [Sov. Phys. Crystallogr. 34 (1989), 85-91].
[18] S.V. Mel'nikova, V.N. Voronov, Specific features of the ferroelastic phase transition in $CsLiS_{(1-z)}Cr_2O_4$ solid solutions, Phys. Solid State 48 (2006) 1786–1790.
[19] N.R. Ivanov, A. Pietraszko, Optical study of the ferroelastic phase transition in $CsLiSO_4$, Phase Transit. 12 (1988) 235–246.
[20] K.S. Aleksandrov, A.V. Zamkov, A.I. Kruglik, $RbMnCl_3$ ferroelastic thermodynamic characteristics, Izv. Akad. Nauk SSSR, Ser. Fiz. 48 (1984) 1175–1179 Bull. Acad. Sci. USSR, Phys. Ser. (English Transl.) 48 (6) (1989) 131–133.
[21] F.J. Schafer, W. Kleeman, High-precision refractive index measurements revealing order parameter fluctuations in $KMnF_3$ and NiO, J. Appl. Phys. 57 (1985) 2606–2612.
[22] S.V. Mel'nikova, V.A. Grankina, Optical investigations of the effect of gradual substitution $NH_4 \rightarrow Cs$ on the ferroelastic phase transition in a $CsLiSO_4$ crystal, Phys. Solid State 46 (2004) 515–520.
[23] E.I. Pogoreltsev, I.N. Flerov, A.V. Kartashev, E.V. Bogdanov, N.M. Laptash, Structural transformation between two cubic phases of $(NH4)_3SnF_7$, J. Fluorine Chem. 168 (2014) 247–250.
[24] A.V. Kartashev, M.V. Gorev, E.V. Bogdanov, I.N. Flerov, N.M. Laptash, Thermal properties and phase transition in the fluoride, $(NH_4)_3SnF_7$, J. Solid State Chem. 237 (2016) 269–273.
[25] E.V. Bogdanov, A.V. Kartashev, E.I. Pogoreltsev, M.V. Gorev, N.M. Laptash, I.N. Flerov, Anomalous behaviour of thermodynamic properties at successive phase transitions in $(NH_4)_3GeF_7$, J. Solid State Chem. 256 (2016) 162–167.
[26] K.S. Aleksandrov, I.N. Flerov, Appricable region of hermodynamical theory for structural phase-ransitions close o tricriical point, Fiz. Tverd. Tela (Leningrad) 21 (2) (1979) 327 [Sov. Phys. Solid State 21 (2), 195 (1979)].